coreceptor in conjunction with the TCR. Additionally, by binding to natural killer (NK) receptors, class I molecules can modulate NK activity (*22*, *23*). Here we describe a third pathway by which class I molecules may affect lymphocyte function, by interacting specifically with CD8αα. By binding to TL independently of the TCR MHC specificity, CD8αα acts semiautonomously and not as a TCR coreceptor. This type of interaction may not be exclusive to IELs, as T cells in other tissues also can express CD8αα (*24*, *25*). With the findings presented here, the possibility must now be entertained that CD8αα molecules could have a regulatory function through high-affinity binding to class I molecules.

References and Notes

1. D. A. Fisher, S. W. D. Hunt, L. Hood, *J. Exp. Med.* **162**, 528 (1985).
2. R. Hershberg *et al.*, *Proc. Natl. Acad. Sci. U.S.A.* **87**, 9727 (1990).
3. M. Teitell *et al.*, *Crit. Rev. Immunol.* **14**, 1 (1994).
4. Soluble TL (*T18^{d}*) heavy chain was amplified by the polymerase chain reaction and cloned ahead of the BirA tag coding sequence into the Sal I/Bam HI sites of the mCD1/β_2-microglobulin (β_2m) pBacp10pH expression vector, replacing the CD1d heavy chain. Baculovirus transfection, recombinant protein production, and biotinylation were done as previously described (*26*). TL tetramers were conjugated to streptavidin Tricolor (Caltag) or Neutravidin-PE (Molecular Probes). Tetramer staining was carried out as described (*26*), with 2.5 to 5 μg of tetramer protein. For blocking, 1 μg of anti-TL antibody 18/20 or 0.5 μg of an CD8α-specific antibody (Caltag) was used; the 53-6.7 CD8α-specific antibody does not block TL tetramer staining.
5. Supplemental web material is available on *Science* Online at www.sciencemag.org/cgi/content/full/294/5548/1936/DC1.
6. H. R. Holcombe *et al.*, *J. Exp. Med.* **181**, 1433 (1995).
7. M. Teitell, M. F. Mescher, C. A. Olson, D. R. Littman, M. Kronenberg, *J. Exp. Med.* **174**, 1131 (1991).
8. CD8αβ$^+$ BI-141 cells (10^7) were surface radiolabeled, lysed in NP-40–containing buffer, and immunoprecipitated with CD8α monoclonal antibody (mAb) 53-6.7, followed by CD8β mAb 53-5.8, or with CD8β followed by CD8α mAb. Immunoprecipitations were carried out with 5 μg of antibody followed by Protein G beads (Pierce). After bead removal, the procedure was repeated three times followed by an incubation with Protein G beads alone to remove any remaining antibody and immunoprecipitation with antibody to the nondepleted CD8. 9. Binding measurements were carried out on a Biacore X instrument (Biacore International AB, Uppsala, Sweden), at 25°C at a 20 μl/min flow rate. Soluble CD8αα or CD8αβ molecules, with a COOH-terminally appended leucine zipper, were captured on flow cell 2 containing the 13A12 leucine zipper–specific antibody (*10*). Flow cell 1 had 13A12 only; the sensograms represent subtracted data (flow cell 2 to flow cell 1). Steady-state binding (R_{eq}) was determined by averaging the plateau response phase of the binding curve. R_{eq} data were plotted against the concentration to determine K_D.
10. P. Kern, R. E. Hussey, R. Spoerl, E. L. Reinherz, H. C. Chang, *J. Biol. Chem.* **274**, 27237 (1999).
11. A. Leishman, O. Naidenko, A. Attinger, F. Koning, H. Cheroutre, unpublished observations.
12. Single-letter abbreviations for the amino acid residues are as follows: A, Ala; C, Cys; D, Asp; E, Glu; F, Phe; G, Gly; H, His; I, Ile; K, Lys; L, Leu; M, Met; N, Asn; P, Pro; Q, Gln; R, Arg; S, Ser; T, Thr; V, Val; W, Trp; and Y, Tyr.
13. *IL-2* release assays were carried out using peptide-pulsed, C57BL/6-derived RMA-H thymoma cells as stimulators, or TL transfectants of these cells and OVA peptide-specific B3Z hybridoma cells and CD8α$^+$-transfected variants (*27*) as the effector cells. CD8$^+$ IELs from OT-1 TCR transgenic mice (*14*) were purified (>90%) with magnetic beads (MACS) coated with CD8α mAb (MiltenyiBiotech, GmbH, Germany) according to the manufacturer's guidelines. Cytokine release by IELs was measured in cultures using OVA peptide–pulsed RMA-S thymoma cells deficient in transporter associated with antigen processing (TAP), or TL transfectants of these cells (*6*). Purified OT-1 IELs were labeled with CFSE and 7.5 to 10 × 10^4 per well were incubated with 10^5 RMA-S cells, RMA-S TL transfectants, or the same cells loaded with OVA peptide. Proliferation was monitored 3 days later by flow cytometry. Sorted CD8αα$^+$ IELs and CD8$^+$ splenocytes of H-Y TCR transgenic RAG $2^{-/-}$ male mice (*15*) were used in a 4-hour ^{51}Cr-release assay, with 5 × 10^3 KCSRNRQYL (H-Y) peptide–loaded RMA-S or RMA-S/TL target cells (*12*). CD8$^+$ normal IELs were sorted using the CD8β antibody, to prevent triggering of CD8αα. Effector cells (10^5 per well) were incubated with 10^5 of CD3ε-specific, antibody–loaded, Fc receptor–positive P815 mastocytoma cells (ATCC), or TL transfectants variants. Alternatively, IELs were cultured in wells coated with 1 μg/ml anti-CD3ε-specific antibody, TL, or CD1d tetramers were added at 10 μg per well per day, and cytokines were measured by ELISA after 72 hours.
14. C. Kurts *et al.*, *J. Exp. Med.* **184**, 923 (1996).
15. D. Cruz *et al.*, *J. Exp. Med.* **188**, 255 (1998).
16. G. F. Gao, B. K. Jakobsen, *Immunol. Today* **21**, 630 (2000).
17. C. N. Levelt *et al.*, *Proc. Natl. Acad. Sci. U.S.A.* **96**, 5628 (1999).
18. H. Cheroutre, A. Leishman, L. Gapin, M. Kronenberg, unpublished results.
19. B. Rocha, P. Vassalli, D. Guy-Grand, *J. Exp. Med.* **173**, 483 (1991).
20. P. J. Morrissey, K. Charrier, D. A. Horovitz, F. A. Fletcher, J. D. Watson, *J. Immunol.* **154**, 2678 (1995).
21. N. J. Davidson *et al.*, *J. Exp. Med.* **184**, 241 (1996).
22. M. C. Mingari *et al.*, *Proc. Natl. Acad. Sci. U.S.A.* **93**, 12433 (1996).
23. M. C. Coles, C. W. McMahon, H. Takizawa, D. H. Raulet, *Eur. J. Immunol.* **30**, 236 (2000).
24. T. Hori, X. Paliard, R. de Waal Malefijt, M. Ranes, H. Spits, *Int. Immunol.* **3**, 737 (1991).
25. A. Chidgey, R. Boyd, *Int. Immunol.* **9**, 1527 (1997).
26. J. Matsuda *et al.*, *J. Exp. Med.* **192**, 741 (2000).
27. J. Karttunen, S. Sanderson, N. Shastri, *Proc. Natl. Acad. Sci. USA* **89**, 6020 (1992).
28. C. M. Micelli, P. von Hoegen, J. R. Parnes, *Proc. Natl. Acad. Sci. U.S.A.* **88**, 2623 (1991).
29. J. D. Altman *et al.*, *Science* **274**, 94, (1996).

30. We thank Marieke Cheroutre for her contribution; S. Jameson, C. Micelli, and L. Madakamutil for helpful discussions; and J. Altman, W. Heath, D. Littman, C. Micelli, S. Schoenberger, and N. Shastri for providing constructs, cell lines, and mice. This work was supported by NIH grants DK54451 and AI50263 (H.C.), CA52511 (M.K.), AI 19807 (E.R.), a Fulbright grant and stipends from the Dutch Organization for Scientific Research and the Child Wellbeing fund (F.K.), and a grant from the Swiss National Fund (A.A.). This is manuscript number 413 of the La Jolla Institute for Allergy and Immunology.

19 June 2001; accepted 2 October 2001

RGS-PX1, a GAP for $G\alpha_s$ and Sorting Nexin in Vesicular Trafficking

Bin Zheng,[1,2]* Yong-Chao Ma,[5]* Rennolds S. Ostrom,[3] Christine Lavoie,[1] Gordon N. Gill,[4,1] Paul A. Insel,[3] Xin-Yun Huang,[5] Marilyn G. Farquhar[1,2]†

Heterotrimeric GTP–binding proteins (G proteins) control cellular functions by transducing signals from the outside to the inside of cells. Regulator of G protein signaling (RGS) proteins are key modulators of the amplitude and duration of G protein–mediated signaling through their ability to serve as guanosine triphosphatase–activating proteins (GAPs). We have identified RGS-PX1, a $G\alpha_s$-specific GAP. The RGS domain of RGS-PX1 specifically interacted with $G\alpha_s$, accelerated its GTP hydrolysis, and attenuated $G\alpha_s$-mediated signaling. RGS-PX1 also contains a Phox (PX) domain that resembles those in sorting nexin (SNX) proteins. Expression of RGS-PX1 delayed lysosomal degradation of the EGF receptor. Because of its bifunctional role as both a GAP and a SNX, RGS-PX1 may link heterotrimeric G protein signaling and vesicular trafficking.

Heterotrimeric G proteins relay extracellular signals initiated by hormones, neurotransmitters, chemokines, and sensory stimuli through G protein–coupled receptors to intracellular effectors and trigger a variety of physiological responses (*1*, *2*). Receptor activation causes dissociation of Gα subunits from Gβγ dimers and subsequent regulation of downstream effectors. Members of the RGS protein family serve as GAPs that attenuate G protein–mediated signal transduction by binding to Gα subunits through a conserved RGS domain and accelerating GTP hydrolysis of Gα subunits (*3*).

The RGS proteins characterized to date are GAPs for G_i, G_q, or $G_{12/13}$ classes of G proteins, but no RGS GAP for $G\alpha_s$ has been found. To identify RGS proteins that might serve as GAPs

[1]Department of Cellular and Molecular Medicine, [2]Department of Pathology, [3]Department of Pharmacology, [4]Department of Medicine, University of California San Diego, La Jolla, CA 92093–0651, USA. [5]Department of Physiology, Weill Medical College of Cornell University, New York, NY 10021, USA.

*These authors contributed equally to this work.
†To whom correspondence should be addressed. E-mail: mfarquhar@ucsd.edu

for $G\alpha_s$, we searched sequence databases with representative RGS domains from the six known mammalian RGS subfamilies and subsequently isolated a cDNA clone encoding a 957–amino acid protein from a human heart cDNA library (*4*) (Fig. 1A), which we named RGS-PX1 based on the presence of both an RGS domain (Fig. 1B) and a Phox (PX) domain (*5*, *6*). RGS-PX1 also contains an NH_2-terminal hydrophobic region (~36 amino acids), a PX-associated domain (PXA) of unknown function (*5*), and several coiled-coil regions (Fig. 1A).

To determine whether RGS-PX1 interacts directly with Gα subunits, bovine brain lysates were incubated with fusion proteins containing glutathione *S*-transferase (GST) and either the RGS domain of RGS-PX1 or RGS4, immobilized on glutathione-agarose beads in the presence of guanosine diphosphate (GDP) and AlF_4^- (*7*), which mimicks the transition state of Gα. RGS-PX1 specifically bound $G\alpha_s$ but not $G\alpha_{i3}$, $G\alpha_q$, or $G\alpha_{12}$ in brain lysates (Fig. 2A), whereas RGS4 bound $G\alpha_i$ and $G\alpha_q$ but not $G\alpha_s$ and $G\alpha_{12}$ as previously reported (*8*, *9*). The specificity of the interaction between RGS-PX1 and $G\alpha_s$ was confirmed by incubating $G\alpha_s$ or $G\alpha_{i1}$ proteins with RGS4 or the RGS domain of RGS-PX1 bound to beads in the presence of GDP or GDP and AlF_4^- (*10*). RGS-PX1 bound the GDP-AlF_4^- form of $G\alpha_s$, whereas RGS4 bound only the GDP-AlF_4^- form of $G\alpha_{i1}$ (Fig. 2B). These data indicate that RGS-PX1 specifically interacts with $G\alpha_s$.

To test whether RGS-PX1 can function as a GAP for $G\alpha_s$, single turnover GTPase assays were performed (*11*, *12*). RGS-PX1 accelerated the catalytic rate of GTP hydrolysis of $G\alpha_s$ at least 20-fold over that of Gαs alone, whereas RGS4 had no effect (Fig. 2C). In the absence of RGS-PX1 or in the presence of RGS4, the half life ($t_{1/2}$) of GTP hydrolysis by $G\alpha_s$ was ~5 min, whereas in the presence of RGS-PX1 it was <15 s, the earliest time point (Fig. 2D). RGS-PX1 had no effect on $G\alpha_{i1}$, whereas RGS4 markedly accelerated the GTP hydrolysis of $G\alpha_{i1}$ (Fig. 2D). These results demonstrate that RGS-PX1 is a GAP for $G\alpha_s$.

To investigate the effects of RGS-PX1 on $G\alpha_s$-mediated signaling, cAMP production was measured in transfected HEK293 cells expressing the β2-adrenergic receptor (β2AR) (*13*). Treatment of cells with the β2AR agonist isoproterenol increased the cellular cAMP level. This increase was reduced (~70%) in cells expressing the RGS domain of RGS-PX1 (Fig. 3A). Additionally, incubation of neonatal rat cardiac membranes with the RGS domain of RGS-PX1 (*13*) reduced isoproterenol-stimulated adenylyl cyclase (AC) activity by ~65% (Fig. 3B). No effect was seen on forskolin-induced cAMP production or on AC activation, which does not require $G\alpha_s$. These data are consistent with the conclusion that RGS-PX1 attenuates $G\alpha_s$-mediated signaling by functioning as a GAP.

RGS-PX1 also contains a PX domain followed by a coiled-coil region (Fig. 1A) often found in SNX proteins, which are involved in vesicular trafficking (*14*–*17*). To determine whether RGS-PX1 can function as a SNX, we examined the effects of overexpressing a fusion protein containing green fluorescence protein (GFP) and RGS-PX1 (GFP-RGS-PX1) on EGF receptor (EGFR) trafficking (*18*). Upon ligand stimulation, EGFR is rapidly internalized, sorted

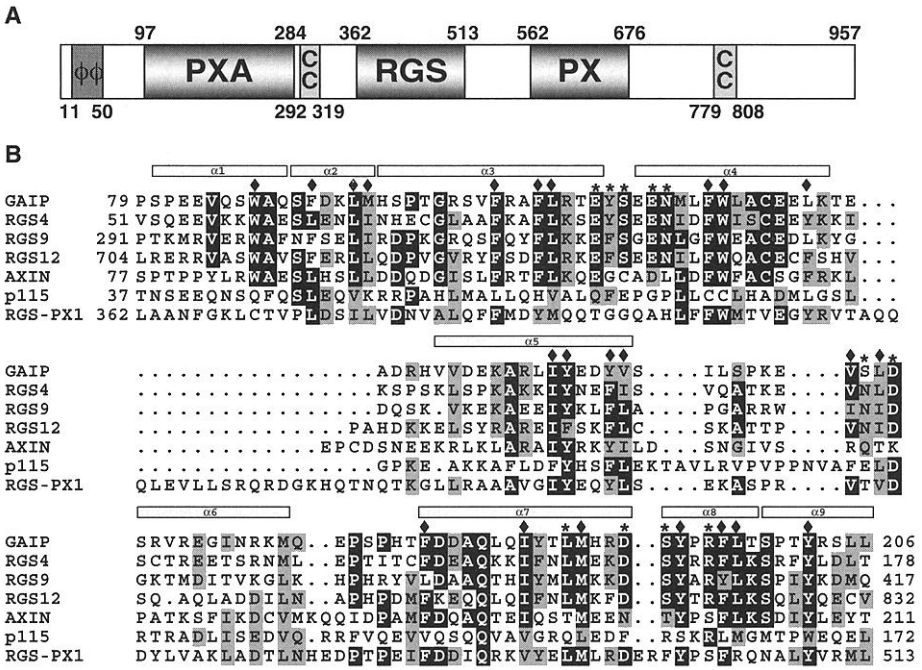

Fig. 1. Structure of RGS-PX1. (**A**) Schematic representation of RGS-PX1. PX, Phox homology domain; PXA, PX-associated domain; CC, coiled-coil regions; ϕ, hydrophobic regions. (**B**) The RGS domain of RGS-PX1 is homologous to those of other RGS proteins (*27*). Conserved residues are shaded in black; similar residues are shaded in gray. The regions containing the alpha helixes (α1 through α9) found in RGS4 are indicated above the sequences. The $G\alpha_{i1}$-contacting (asterisks) and hydrophobic core residues (diamonds) of RGS4 are also indicated. p115, p115RhoGEF.

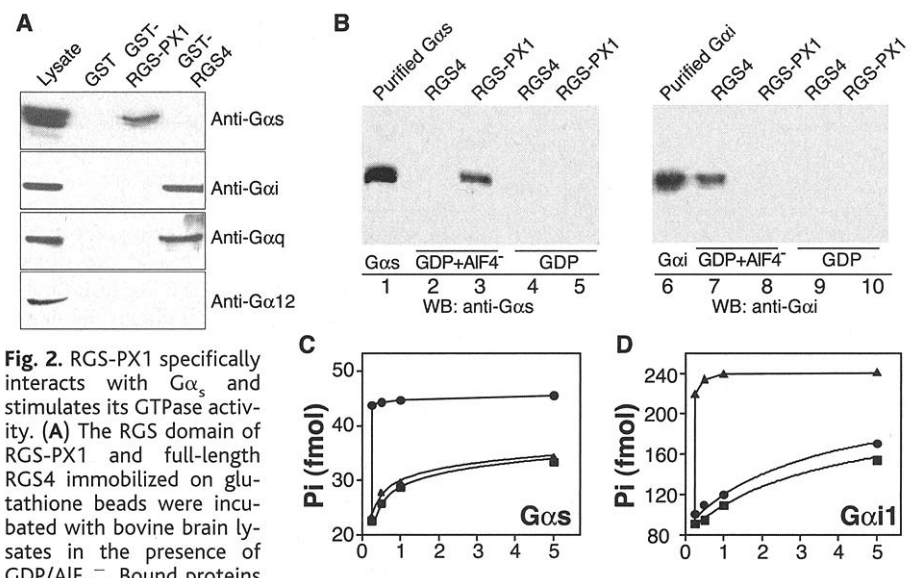

Fig. 2. RGS-PX1 specifically interacts with $G\alpha_s$ and stimulates its GTPase activity. (**A**) The RGS domain of RGS-PX1 and full-length RGS4 immobilized on glutathione beads were incubated with bovine brain lysates in the presence of GDP/AlF_4^-. Bound proteins were analyzed by immunoblotting for the indicated Gα subunits. (**B**) RGS domains of RGS-PX1 and RGS4 immobilized on Ni-NTA beads were incubated with purified recombinant $G\alpha_s$ (lanes 1 through 5) or $G\alpha_{i1}$ (lanes 6 through 10) in the presence of GDP/AlF_4^- (lanes 2, 3, 7, and 8) or GDP alone (lanes 4, 5, 9, and 10) and analyzed as in (A). WB, Western blotting. Lanes 1 and 6 were loaded with 0.1 μg of $G\alpha_s$ or $G\alpha_{i1}$. (**C**) RGS-PX1 (400 nM, circles) but not RGS4 (400 nM, triangles) increases the rate of GTP hydrolysis of $G\alpha_s$ over $G\alpha_s$ alone (squares). (**D**) RGS4 (250 nM, triangles), but not RGS-PX1 (800 nM, circles), increases the rate of GTP hydrolysis of $G\alpha_{i1}$ over $G\alpha_{i1}$ alone (squares). The hydrolysis reaction contained 80 nM $G\alpha_s$ (C) or 60 nM $G\alpha_{i1}$ (D) and was performed on ice. Data shown are representative of at least three independent experiments.

in endosomes, and targeted to lysosomes for degradation. Ligand-dependent EGFR degradation was delayed in transfected HEK293 cells expressing GFP-RGS-PX1 (Fig. 4A), which suggests inhibition of lysosomal targeting and/or degradation of EGFR. Because EGFR trafficking to endosomes is important for regulating receptor signaling, we assessed whether expression of GFP-RGS-PX1 influences EGF-dependent mitogen-activated protein kinase (MAPK) activation (*18*). In controls, phosphorylation of ERK1 and ERK2 increased 5 min after EGF addition and decreased progressively from 30 to 60 min (Fig. 4B), in keeping with the observed rapid degradation of active EGFR (Fig. 4A). In contrast, cells transfected with GFP-RGS-PX1 showed sustained activation of ERK1 and ERK2 at 30 and 60 min (Fig. 4B). This prolonged EGF signaling correlates well with the delay in EGFR degradation, supporting a regulatory role for RGS-PX1 in EGFR trafficking and signaling.

The PX domain has recently been shown to be a phosphoinositide-binding domain involved in membrane targeting (*17*, *19*); and in the case of SNX3, the interaction between the PX domain and phosphoinositides is important for its function (*17*). To examine its phosphoinositide-binding properties, we performed a protein-lipid binding assay with a GST fusion protein containing the PX domain of RGS-PX1 (*18*) and found that it bound strongly to PtdIns(3)P and PtdIns(5)P and weakly to PtdIns(3,5)P2 and PtdIns(4)P, but not to other phosphoinositides or other phospholipids (Fig. 4C).

GFP-RGS-PX1 also colocalized with the early endosome marker EEA1 in Cos-7 cells (*18*) (Fig. 4D). PtdIns(3)P is highly enriched in early endosomes (*17*), whereas the subcellular localization of PtdIn(5)P has not been established. These results suggest that RGS-PX1 is a functional SNX that could regulate EGFR trafficking and signaling, probably through the interaction of its PX domain with phosphoinositides in endosomes.

As a GAP for $G\alpha_s$, RGS-PX1 likely contributes to the regulation of cellular responses mediated by $G\alpha_s$. $G\alpha_s$ stimulates adenylyl cyclases, L-type calcium channels, and Src kinase; inhibits cardiac sodium channels; and is involved in many cellular responses, including cell growth, differentiation and proliferation, membrane trafficking, cardiac contraction and relaxation, hormone secretion, and learning and memory (*1*, *2*, *20*). The existence of RGS-PX1 as a GAP for $G\alpha_s$ may explain the difference between the slow rate of GTP hydrolysis of $G\alpha_s$ in vitro and its rapid rate of deactivation under certain physiological conditions (*21*). The specificity of the interaction between $G\alpha$ subunits and RGS proteins is very likely determined by the primary sequences of RGS domains and $G\alpha$ proteins. It has been suggested that the major barrier to $G\alpha_s$ interaction with other RGS proteins is Asp^{229} of $G\alpha_s$ (*3*). Substitution of this residue with the corresponding Ser^{206} of $G\alpha_i$ enabled the mutated $G\alpha_s$ to bind to RGS4 and RGS16. It is known from the crystal structure of the $G\alpha_{i1}$-RGS4 complex that Ser^{206} of $G\alpha_{i1}$ interacts with Glu^{126} and Asn^{128} of RGS4 (*3*). In RGS-PX1, Arg^{457} and Thr^{459} occupy these positions. These two nonconserved amino acid substitutions suggest that Arg^{457} and Thr^{459} in RGS-PX1 might contribute to the specificity of $G\alpha_s$-RGS interaction.

A unique feature of RGS-PX1 is its dual role as both a GAP and a SNX. Whereas the RGS domain of RGS-PX1 is responsible for its GAP activity for $G\alpha_s$, the PX domain and the

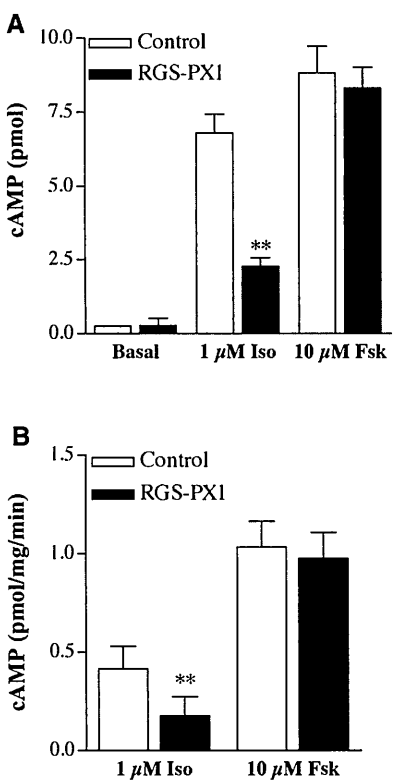

Fig. 3. RGS-PX1 attenuates $G\alpha_s$-mediated signaling. (**A**) RGS-PX1 inhibits isoproterenol (Iso)– but not forskolin (Fsk)–induced cAMP production. HEK293 cells were transfected with the RGS domain of RGS-PX1 or with empty vector together with β2AR. (**B**) RGS-PX1 inhibits Iso- but not Fsk-stimulated AC activity in neonatal rat cardiac myocyte membranes. Membranes were incubated for 5 min on ice with 50 nM RGS domain of RGS-PX1 or with vehicle before AC activity was measured. cAMP production over basal production (no agonist) is shown. Data are expressed as the mean ± SEM of three experiments. $^{**}P < 0.005$ by paired *t* test.

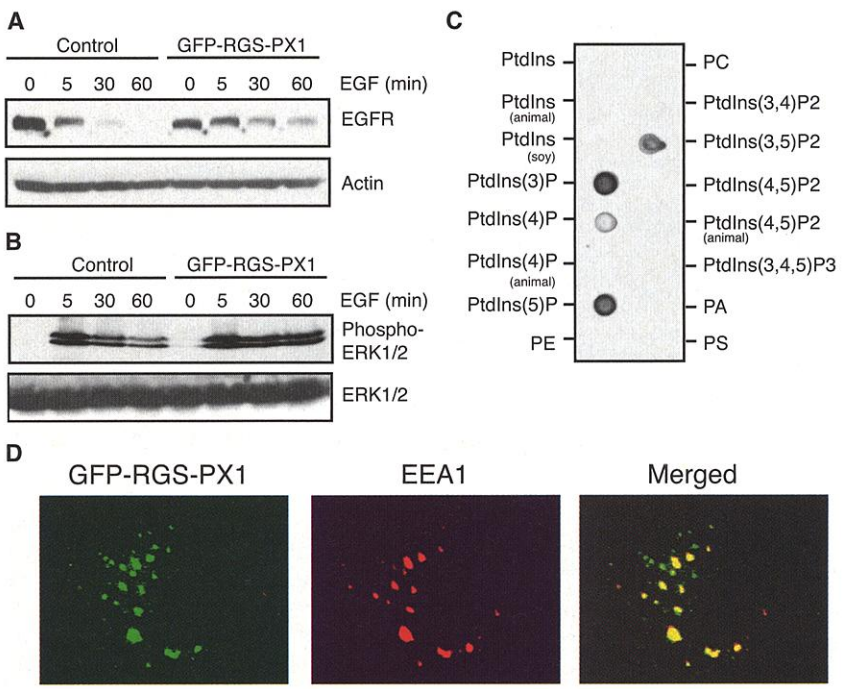

Fig. 4. RGS-PX1 is a functional sorting nexin. (**A**) Expression of GFP-RGS-PX1 causes a delay in the degradation of EGFR in HEK293 cells. Cells transfected with GFP-RGS-PX1 or with empty GFP vector were treated with EGF for the indicated times, followed by immunoblotting with antibodies against EGFR or actin. Data shown are representative of at least three independent experiments. (**B**) Expression of GFP-RGS-PX1 in HEK293 cells inhibits down-regulation of EGF-dependent MAPK activation. Cells transfected with GFP-RGS-PX1 or with empty GFP vector were treated with EGF for the indicated times, and activation of MAPK (phospho-ERK1/2) was assessed by immunoblotting. Data shown are representative of at least three independent experiments. (**C**) The PX domain of RGS-PX1 binds strongly to PtdIns(3)P and PtdIns(5)P and weakly to PtdIns(3,5)P2 and PtdIns(4)P. A GST fusion protein containing the PX domain of RGS-PX1 was used in a protein-lipid overlay. Bound proteins were detected by immunoblotting with antibody to GST. PA, phosphatidic acid; PC, phosphatidylcholine; PE, phosphatidylethanolamine; PS, phosphatidylserine. (**D**) GFP-RGS-PX1 colocalizes with EEA1 in Cos7 cells. Right panel, merged images. Yellow indicates overlap.

COOH-terminal coiled-coil region, which are shared with other SNX proteins, are most likely responsible for its SNX function. The presence of both activities in one molecule makes RGS-PX1 an ideal bridge between G protein signaling and regulation of vesicular trafficking.

References and Notes

1. A. G. Gilman, *Annu. Rev. Biochem.* **56**, 615 (1987).
2. A. J. Morris, C. C. Malbon, *Physiol. Rev.* **79**, 1373 (1999).
3. L. De Vries, B. Zheng, T. Fischer, E. Elenko, M. G. Farquhar, *Annu. Rev. Pharmacol. Toxicol.* **40**, 235 (2000).
4. Initially we identified a human cDNA clone KIAA0713 (GenBank accession number BAA34433) and several expressed sequence tags encoding an RGS protein through a BLAST search of GenBank (National Center for Biotechnology Information). A full-length cDNA (RGS-PX1, GenBank accession number AF420470) was obtained by screening a human heart cDNA library (Stratagene) with a fragment corresponding to the putative RGS domain of KIAA0713 and subsequent 5′ rapid amplification of cDNA ends with human heart Marathon-ready cDNA (Clontech). RGS-PX1 appears to be an alternatively spliced form of KIAA0713, with a longer COOH-terminal region. The COOH-terminal region of RGS-PX1 encoding the last 362 residues is identical to a partial cDNA encoding SNX13 (GenBank accession number AAD27835). Domain analysis was done with the SMART database (*5*). Sequence alignment and shading were conducted with the ClustalW and MacBoxshade programs, respectively. MacVector software (Oxford Molecular, Madison, WI) was used for transmembrane region prediction.
5. C. P. Ponting, J. Schultz, F. Milpetz, P. Bork, *Nucleic Acids Res.* **27**, 229 (1999).
6. Supplementary Web material is available on *Science* Online at www.sciencemag.org/cgi/content/full/294/5548/1939/DC1.
7. The RGS domain of RGS-PX1 (residues 327 through 526) or full-length RGS4 was expressed in *Escherichia coli* as GST- or His-tagged protein with the pGEX-KG (Pharmacia) and pET28 (Novagen) vectors, respectively. Recombinant proteins were purified as described (*22*). For pulldown assays on brain lysates, GST-RGS-PX1, GST-RGS4, or GST (~5 μg) on glutathione-agarose beads (Sigma) were incubated overnight with ~10 mg of bovine brain lysate in buffer A [20 mM tris-HCl (pH 8.0), 100 mM NaCl, 2 mM $MgSO_4$, 5 mM β-mercaptoethanol, 0.05% C12E10, and 5% glycerol] containing 100 μM GDP in the presence of 30 μM $AlCl_3$ and 10 μM NaF at 4°C as described (*23*). Bound proteins were analyzed by immunoblotting with affinity-purified antibody to $G\alpha_{i3}$ (EC) and $G\alpha_q$ (QL) and with protein A–purified anti-$G\alpha_s$ and anti-$G\alpha_{12}$ immunoglobulin G's (IgG's) (Calbiochem).
8. N. Watson, M. E. Linder, K. M. Druey, J. H. Kehrl, K. J. Blumer, *Nature* **383**, 172 (1996).
9. J. R. Hepler, D. M. Berman, A. G. Gilman, T. Kozasa, *Proc. Natl. Acad. Sci. U.S.A.* **94**, 428 (1997).
10. Two micrograms of purified His-tagged RGS domain of RGS-PX1 or full-length RGS4 bound to Ni-NTA-agarose beads and 0.1 μg of $G\alpha_s$ or $G\alpha_{i1}$ were incubated at room temperature for 5 min in 500 μl of buffer B [20 mM tris-HCl (pH 8.0), 0.5 mM EDTA, 20% glycerol, 1 mM dithiothreitol (DTT), 0.2% NP-40, and 0.5 mM phenylmethylsulfonyl fluoride] containing 100 μM GDP in the presence of 30 μM $AlCl_3$ and 10 μM NaF as described (*24*). The reaction mixture was then washed (three times) with 1 ml of buffer B with 100 mM KCl. Bound $G\alpha_s$ and $G\alpha_{i1}$ were analyzed by immunoblotting with specific antibodies (*7*).
11. Hydrolysis of GTP and purification of $G\alpha_s$ and $G\alpha_{i1}$ were done as described (*24*, *25*). $G\alpha_s$ or $G\alpha_{i1}$ (200 nM) was loaded with [γ-^{32}P]GTP by incubation for 15 min at 30°C in 50 mM NaHepes (pH 8.0), 10 mM EDTA, 5 mM DTT, and 2 μM [γ^{32}-P]GTP (~10,000 counts per min per pmol) in the absence of Mg^{2+} and presence of EDTA to prevent GTP hydrolysis. We typically obtained 15 to 30% loading. GTPase assays were performed on ice in an attempt to capture the initial phase of GTP hydrolysis (*25*). One round of hydrolysis of the prebound [γ-^{32}P]GTP was started by addition of $MgSO_4$ and unlabeled GTP to final concentrations of 20 mM and 100 μM, respectively. Excess unlabeled GTP was included to prevent rebinding of [γ-^{32}P]GTP. Final concentrations of $G\alpha_s$ or $G\alpha_{i1}$ were 80 and 60 nM, respectively. In some cases, 400 nM purified His-tagged RGS domain of RGS-PX1 or full-length RGS4 was included. At the indicated times, aliquots (10 μl) were removed and added to 260 μl of 5% w/v Norit A charcoal and [^{32}P]P_i was counted by liquid scintillation.
12. D. M. Berman, T. Kozasa, A. G. Gilman, *J. Biol. Chem.* **271**, 27209 (1996).
13. HEK293T cells in six-well plates were transfected using calcium phosphate with 1 μg of pCMV-β2AR and 4 μg of pCDNA3-FLAG-RGS-PX1-RGS or pCDNA3. Forty-eight hours after transfection, cells were serum-starved overnight, treated with 1 μM isobutyl methylxanthine for 30 min, and stimulated with 50 μM isoproterenol or 100 μM forskolin for 3 min. Cells were then lysed and cAMP accumulation was measured with the cAMP enzyme immunoassay system (Amersham Pharmacia) according to the manufacturer's protocol. For assay of AC activity, membranes from neonatal rat cardiac myocytes were prepared as described (*26*). His-tagged RGS domain of RGS-PX1 (150 nM) or vehicle was added to membranes for 5 min on ice and diluted 1:3 (50 nM final concentration) with AC assay reactants. Reactants were incubated for 10 min at 30°C, boiled, and assayed for cAMP content by radioimmunoassay (*26*).
14. R. C. Kurten, D. L. Cadena, G. N. Gill, *Science* **272**, 1008 (1996).
15. B. F. Horazdovsky *et al.*, *Mol. Biol. Cell* **8**, 1529 (1997).
16. C. R. Haft, M. de la Luz Sierra, V. A. Barr, D. H. Haft, S. I. Taylor, *Mol. Cell. Biol.* **18**, 7278 (1998).
17. Y. Xu, H. Hortsman, L. Seet, S. H. Wong, W. Hong, *Nature Cell Biol.* **3**, 658 (2001).
18. HEK293 cells were transfected using calcium phosphate (>50% transfection efficiency) with GFP-RGS-PX1, RGS-PX1 (residues 257 through 957) in pEGFP-C1 vector (Clontech), or empty vector together with EGFR. Twenty-four hours after transfection, cells were serum-starved for 16 hours and lysed at different times after addition of 10 nM EGF (Molecular Probes). Fifty micrograms of cell lysate was analyzed by immunoblotting with antibodies to EGFR (*14*), actin (Sigma), phosphoERK1/2, and ERK1/2 (Cell Signaling Technology, Beverly, MA). Protein-lipid overlays were performed essentially as described (*19*) with the use of PIP-strips (Echelon Research Laboratories, Salt Lake City, UT), a GST fusion protein (0.5 μg/ml) of the PX domain of RGS-PX1 (residues 562 through 676), and monoclonal antibody to GST (Santa Cruz Biotechnology). For immunofluorescence, Cos-7 cells were transiently transfected with GFP-RGS-PX1 by means of Fugene 6 (Roche). Twenty-four hours after transfection, cells were fixed in 2% paraformaldehyde, permeabilized (0.1% Triton-X100), and incubated with antibody to EEA1 (Transduction Laboratories, Lexington, KY), followed by Alexa 594 goat anti-rabbit IgG as described (*22*).
19. M. L. Cheever *et al.*, *Nature Cell Biol.* **3**, 613 (2001).
20. J. B. Helms, *FEBS Lett.* **369**, 84 (1995).
21. A. Yatani, A. M. Brown, *Science* **245**, 71 (1989).
22. B. Zheng, D. Chen, M. G. Farquhar, *Proc. Natl. Acad. Sci. U.S.A.* **97**, 3999 (2000).
23. C. V. Carman *et al.*, *J. Biol. Chem.* **274**, 34483 (1999).
24. Y. C. Ma, J. Huang, S. Ali, W. Lowry, X. Y. Huang, *Cell* **102**, 635 (2000).
25. C. Kleuss, A. S. Raw, E. Lee, S. R. Sprang, A. G. Gilman, *Proc. Natl. Acad. Sci. U.S.A.* **91**, 9828 (1994).
26. R. S. Ostrom *et al.*, *J. Biol. Chem.* Papers in Press, published 2001 as 10.1074/jbc.M105348200.
27. Single-letter abbreviations for the amino acid residues are as follows: A, Ala; C, Cys; D, Asp; E, Glu; F, Phe; G, Gly; H, His; I, Ile; K, Lys; L, Leu; M, Met; N, Asn; P, Pro; Q, Gln; R, Arg; S, Ser; T, Thr; V, Val; W, Trp; and Y, Tyr.

28. We thank T. Nagase (Kazusa DNA Research Institute, Japan) for the KIAA0713 cDNA clone and A. Spiegel (NIH) for anti-$G\alpha_i$ EC and anti-$G\alpha_q$ QL IgGs. Supported by NIH grants CA58689 and DK17780 (M.G.F.), AG14563 and GM56904 (X.-Y.H.), and HL53773 and HL63885 (P.A.I.) and a fellowship from the Canadian Institutes of Health Research (C.L.).

25 July 2001; accepted 9 October 2001

Phosphatidic Acid–Mediated Mitogenic Activation of mTOR Signaling

Yimin Fang, Montserrat Vilella-Bach, Rebecca Bachmann, Asa Flanigan, Jie Chen*

The mammalian target of rapamycin (mTOR) governs cell growth and proliferation by mediating the mitogen- and nutrient-dependent signal transduction that regulates messenger RNA translation. We identified phosphatidic acid (PA) as a critical component of mTOR signaling. In our study, mitogenic stimulation of mammalian cells led to a phospholipase D–dependent accumulation of cellular PA, which was required for activation of mTOR downstream effectors. PA directly interacted with the domain in mTOR that is targeted by rapamycin, and this interaction was positively correlated with mTOR's ability to activate downstream effectors. The involvement of PA in mTOR signaling reveals an important function of this lipid in signal transduction and protein synthesis, as well as a direct link between mTOR and mitogens. Furthermore, these studies suggest a potential mechanism for the in vivo actions of the immunosuppressant rapamycin.

The mammalian target of rapamycin (mTOR; also named FRAP or RAFT1) (*1*–*3*) belongs to the family of phosphatidylinositol kinase–like kinases (PIKK) (*4*). The mTOR homologs in *Saccharomyces cerevisae*, Tor1p and Tor2p, control a wide range of growth-related cellular processes, including transcription, translation, and reorganization of the actin cytoskeleton (*5*).